

Elsevier Editorial System(tm) for Journal of Magnetism and Magnetic Materials
Manuscript Draft

Manuscript Number:

Title: Calculation of nanoparticle capture efficiency in magnetic drug targeting

Article Type: Regular Submission

Keywords: magnetic drug targeting, high gradient magnetic separation (HGMS),
magnetic nanoparticles, simulation, magnetic seed

Corresponding Author: Dr Patrick Joseph Cregg, PhD

Corresponding Author's Institution: Waterford Institute of Technology

First Author: Patrick Joseph Cregg, PhD

Order of Authors: Patrick Joseph Cregg, PhD; Kieran Murphy, PhD; Adil Mardinoglu, BEng

Abstract: The magnetic targeted drug delivery system of Avil'es, Ebner and Ritter, which uses high gradient magnetic separation (HGMS) is considered. In that model large ferromagnetic particles are used as seeds to aid collection of multiple domain nanoparticles (radius ≈ 200 nm). Here, in contrast, single domain magnetic nanoparticles (radius in 20-100 nm) are considered and the Langevin function is used to describe the magnetization. Simulations based on this model were performed using the open source C++ finite volume library OpenFOAM. The simulations indicate that use of the Langevin function predicts greater collection efficiency than might be otherwise expected.

Dr PJ Cregg
Materials Characterisation & Processing Group
Waterford Institute of Technology
Waterford
Ireland
picregg@wit.ie
tel ++353 51 302631
mobile ++353 87 6798710

Dear Prof Chantrell,

Please find attached a copy of *Calculation of nanoparticle capture efficiency in magnetic drug targeting* by P.J. Cregg , Kieran Murphy, Adil Mardinoglu which I hope will be of interest to readers of the *Journal of Magnetism and Magnetic Materials*.

Best regards
Dr P J Cregg

1 Calculation of nanoparticle capture efficiency 2 in magnetic drug targeting

3 P.J. Cregg^{*}, Kieran Murphy, Adil Mardinoglu

4 *Materials Characterisation and Processing Group, Waterford Institute of*
5 *Technology, Waterford, Ireland*

6 Abstract

7 The magnetic targeted drug delivery system of Avilés, Ebner and Ritter, which uses
8 high gradient magnetic separation (HGMS) is considered. In that model large fer-
9 romagnetic particles are used as seeds to aid collection of multiple domain nanopar-
10 ticles (radius ≈ 200 nm). Here, in contrast, single domain magnetic nanoparticles
11 (radius in 20–100 nm) are considered and the Langevin function is used to describe
12 the magnetization. Simulations based on this model were performed using the open
13 source C++ finite volume library OpenFOAM. The simulations indicate that use of
14 the Langevin function predicts greater collection efficiency than might be otherwise
15 expected.

16 *Key words:* magnetic drug targeting, high gradient magnetic separation (HGMS),
17 magnetic nanoparticles, simulation, magnetic seed

18 *PACS:* 47.63.mh, 47.63.-b, 87.85.gf

* Corresponding author.

Email address: pjcregg@wit.ie (P.J. Cregg).

19 **1 Introduction**

20 Magnetic nanoparticles continue to offer much promise as carriers in drug
21 targeting systems [1, 2]. That the force exerted on an individual particle
22 is determined by the gradient of the field and not simply the field is well
23 known [1, 3–8]. As has been pointed out by several authors [3–8] this may
24 inhibit the targeting, solely by means of external permanent magnets, of ar-
25 eas deep within the body. With this in mind, the implanting of ferromagnetic
26 materials, such as wires, seeds or stents, in blood vessels has been proposed
27 by some authors [4–7], in order to create large localised gradients within the
28 vessels. Berry [2] has suggested that magnetic nanoparticles with radius of the
29 order of 50 nm may have advantages as drug carriers, and here these are taken
30 as the carriers. For a related problem, Furlani and Furlani [9] have developed
31 a model for which it was possible to obtain an analytical expression for the
32 behaviour of multifunctional particles. In contrast, the approach taken here is
33 largely numerical in that while the magnetic field is obtained from an analyti-
34 cal expression both the fluid flow and resulting particle trajectories are obtain
35 using OpenFOAM a finite volume simulation C++ library.

36 **2 Outline of Model**

37 The model of Avilés, Ebner and Ritter [10], is considered, which uses ferro-
38 magnetic material, to create a localised field gradient, at the desired site in
39 the body. This ferromagnetic material, termed seed, has a radius of the or-
40 der of $1\ \mu\text{m}$. The model treats the behaviour of magnetic particles under the

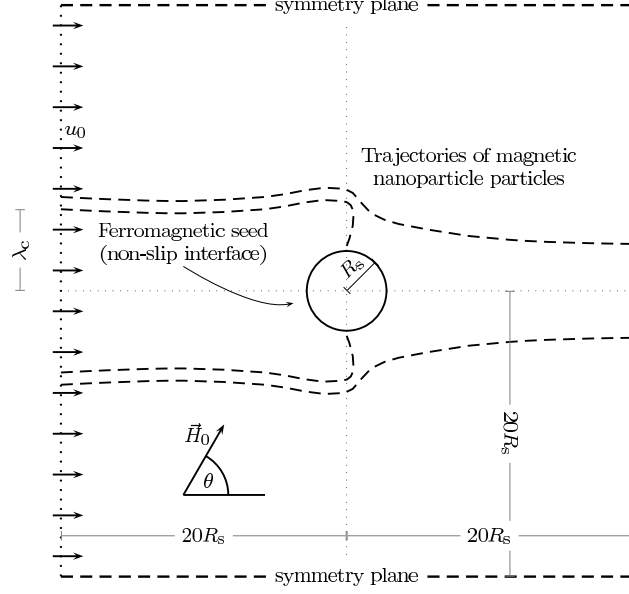


Fig. 1. Schematic diagram of the control volume, CV, used in determining the capture radius, λ_c , of the superparamagnetic single-domain nanoparticles.

41 influence of Stokes drag and the magnetic force. The Stokes drag is given by

$$\vec{F}_s = 6\pi\eta_b R_p (\vec{v}_b - \vec{v}_p), \quad (1)$$

42 where η_b is the viscosity of the blood, R_p the radius of the particle, and \vec{v}_b
 43 and \vec{v}_p are the velocities of the blood and the particle respectively. The blood
 44 velocity, \vec{v}_b , is determined by solving the appropriate Navier-Stokes equations.

45 The magnetic force is determined by

$$\vec{F}_m = (\vec{m} \cdot \nabla) \vec{B}, \quad (2)$$

46 where \vec{B} is the resulting magnetic flux density (due to the external magnetic
 47 field \vec{H} and the presence of the seed) and \vec{m} is the magnetic moment of the
 48 particle. We follow Avilés *et al.* [10] and consider the effect of a magnetisable
 49 seed placed in the blood flow as indicated in Fig. 1. The magnetisation of the
 50 seed can be calculated from

$$M_{\text{seed}} = 2\alpha_{\text{seed}}H_0, \quad (3)$$

51 where α_{seed} is the demagnetising factor for an infinitely long cylinder in a
 52 perpendicular field taken as

$$\alpha_{\text{seed}} = \min \left(\frac{\chi_{\text{seed},0}}{2 + \chi_{\text{seed},0}}, \frac{M_{\text{seed},s}}{2H_0} \right), \quad (4)$$

53 where $\chi_{\text{seed},0}$ and $M_{\text{seed},s}$ are the zero field susceptibility and saturation mag-
 54 netisation of the ferromagnetic seed respectively, and H_0 is the magnitude of
 55 the externally applied homogeneous field. In the model of Avilés *et al.* mi-
 56 croparticles were considered, where the axis of the moment \vec{m} lay along that
 57 of \vec{B} , and the magnetisation increased with applied field, after accounting for
 58 demagnetising. In contrast, nanoparticles of diameter < 100 nm are typically
 59 superparamagnetic single domains. Accounting for thermal agitation, their
 60 average magnetisation is given by the Langevin function [3, 8, 11, 12]

$$L(\beta) = \coth(\beta) - \frac{1}{\beta}, \quad (5)$$

61 with Langevin argument

$$\beta = \frac{\mu_0 \omega_{\text{fm,p}} V_p M_{\text{fm,p,s}} H}{kT}, \quad (6)$$

62 where μ_0 is the magnetic permeability of free space, $\omega_{\text{fm,p}}$ is the volume fraction
 63 of ferromagnetic material in the particle, V_p is the particle volume, $M_{\text{fm,p,s}}$ the
 64 (volume) saturation magnetisation, k is Boltzmann's constant and T is the
 65 absolute temperature, so that \vec{m} can be written as

$$\vec{m} = \omega_{\text{fm,p}} V_p M_{\text{fm,p,s}} L(\beta) \frac{\vec{B}}{|\vec{B}|}. \quad (7)$$

66 The value of \vec{B} , required to calculate the magnetic force as given by Eqs. (2)
 67 and (7), is calculated from solving the Laplace equation as outlined in Sec-
 68 tion 4.

69 **3 Blood flow — the Navier-Stokes equations**

70 Following the notation of Avilés *et al.* [10] we write the blood velocity \vec{v}_b and
71 the pressure P for a incompressible, Newtonian fluid at steady state. We have
72 the continuity equation

$$\nabla \cdot \vec{v}_b = 0, \quad (8)$$

73 and the Navier-Stokes equation

$$\rho_b[(\vec{v}_b \cdot \nabla \vec{v}_b)] = \nabla P + \eta_b \nabla^2 \vec{v}_b, \quad (9)$$

74 where ρ_b is the density of the blood. To solve Eqs. (8) and (9), a uniform inlet
75 velocity profile is assumed at the inlet control volume (CV) such that

$$\vec{v}_b = \begin{pmatrix} u_0 \\ 0 \end{pmatrix}, \quad (10)$$

76 where u_0 is the inlet blood velocity. Non-slip boundary conditions are applied
77 at the seed surface in contact with the bloodstream. In addition, symmetry
78 boundary conditions are applied at the upper and lower CV boundaries to
79 maintain the constant flow profile and atmospheric pressure is assumed at
80 the outlet of the CV to satisfy the boundary condition on pressure. Other
81 assumptions include isothermal, single-phase, incompressible, Newtonian fluid
82 flow as used by Avilés *et al.* [10].

83 **4 The magnetic force — the scalar magnetic potential**

84 The second part of this model involves the scalar magnetic potential, ϕ , which
85 satisfies the Laplace equation over two con-joined regions: inside the seed and

86 outside the seed. From the scalar potential, we can obtain the magnetic flux
 87 density, \vec{B} , as required, through

$$\vec{B} = -\mu_0 \nabla \phi. \quad (11)$$

88 Thus for the two regions, within the seed and the rest of the space we have
 89 respectively \vec{B}_{seed} and \vec{B}_{space} as

$$\vec{B}_{\text{seed}} = -\mu_0(\vec{m}_{\text{seed}} + \vec{H}_0 - \nabla \phi_{\text{seed}}), \quad (12)$$

$$\vec{B}_{\text{space}} = -\mu_0(\vec{H}_0 - \nabla \phi_{\text{space}}), \quad (13)$$

90 where ϕ_{seed} and ϕ_{space} represent the scalar magnetic potential within the seed
 91 and in the space outside the seed respectively. Here \vec{m}_{seed} is the induced mag-
 92 netisation of the seed and \vec{H}_0 is the applied homogenous magnetic field given
 93 by

$$\vec{H}_0 = \begin{pmatrix} H_0 \cos \theta \\ H_0 \sin \theta \end{pmatrix}, \quad (14)$$

94 where θ is the angle from the positive x -axis. Laplace's equation for the scalar
 95 potential is solved analytically by separation of variables. Firstly, the normal
 96 component of the magnetic flux and potential are both assumed to be con-
 97 tinuous across the seed-blood interface. Secondly, the scalar potential should
 98 tend towards zero far away from the seed. The required analytical solution is

$$\phi_{\text{seed}} = H_0 \frac{\mu_r - 1}{\mu_r + 1} (x \cos \theta + y \sin \theta), \quad \phi_{\text{space}} = H_0 \frac{\mu_r - 1}{\mu_r + 1} \frac{x \cos \theta + y \sin \theta}{x^2 + y^2}, \quad (15)$$

99 where μ_r is the relative permeability of the ferromagnetic seeds.

100 **5 Velocity equations, streamlines and capture cross section**

101 Considering the forces, the velocity equations can be obtained through com-
 102 bining the hydrodynamic and magnetic velocities [10],

$$\vec{v}_p = \vec{v}_b + \frac{1}{2} V_m \frac{R_{\text{seed}}}{M_{\text{seed},s} H_f} \nabla (\vec{H}_f \cdot \vec{H}_f), \quad (16)$$

103 where R_{seed} is the seed radius and \vec{H}_f is the total magnetic field at the location
 104 of the magnetic drug carrier particle and is given by

$$\vec{H}_f = \vec{H}_0 - \nabla \phi_{\text{space}}. \quad (17)$$

105 Here the magnitude of the total magnetic field H_f is given by $\sqrt{\vec{H}_f \cdot \vec{H}_f}$ so that

$$H_f = \sqrt{\left(H_0 \cos \theta - \frac{\partial \phi_{\text{space}}}{\partial x} \right)^2 + \left(H_0 \sin \theta - \frac{\partial \phi_{\text{space}}}{\partial y} \right)^2}. \quad (18)$$

106 The magnetic velocity, \vec{v}_m , is given by

$$\vec{v}_m = \frac{2}{9} \frac{R_p^2}{R_{\text{seed}}} \frac{\mu_0}{\eta_b} \omega_{\text{fm},p} M_{\text{seed},s} M_{\text{fm},p,s} L(\beta). \quad (19)$$

107 The volume fraction of ferromagnetic material $\omega_{\text{fm},p}$ in the magnetic drug
 108 carrier particle is related to its weight fraction $x_{\text{fm},p}$ through [5]

$$\omega_{\text{fm},p} = \frac{x_{\text{fm},p}}{x_{\text{fm},p} + (1 - x_{\text{fm},p}) \rho_{\text{fm},p} / \rho_{\text{pol},p}}, \quad (20)$$

109 where $\rho_{\text{fm},p}$ is the density of the ferromagnetic material in the magnetic drug
 110 carrier particle and $\rho_{\text{pol},p}$ is the density of the polymer material in the magnetic
 111 drug carrier particle.

112 Finally, the particle trajectories are obtained from evaluating the streamline
 113 function

$$\frac{\partial \psi}{\partial y} = -v_{p,x}, \quad (21)$$

114

$$\frac{\partial \psi}{\partial x} = -v_{p,y}, \quad (22)$$

115 where ψ is the stream function, and $v_{p,x}$ and $v_{p,y}$ are the components of \vec{v}_p
 116 which are given by Eq. (16). The system performance of this model is calcu-
 117 lated in terms of the capture cross section, λ_c , defined as

$$\lambda_c = \frac{y_c}{R_{\text{seed}}}, \quad (23)$$

118 where y_c is the capture radius of the ferromagnetic seed. The capture radius,
 119 y_c , is defined by the location of the streamline at the entrance to the CV of
 120 the last magnetic drug carrier particle captured to the seed. All calculations
 121 were performed using the open-source software finite volume library Open-
 122 FOAM [13].

123 6 Results and Discussions

124 In this simulation iron is used as the magnetic drug carrier particle and SS 409
 125 is used as the seed ferromagnetic material. The streamline functions for the
 126 capture of nanoparticles are presented in Fig. 2 for particle radius $R_p = 50$ nm,
 127 containing 40 wt% iron ($x_{\text{fm,p}} = 0.4$), under the influence of homogenous mag-
 128 netic field $\mu_0 H_0$ oriented perpendicularly to the flow ($\theta = \pi/2$) with magni-
 129 tudes of 0.0 to 0.6 T. In this a single SS409 ferromagnetic seed, with $1 \mu\text{m}$
 130 radius is located in the CV. The resulting capture cross-section, λ_c , is calcu-
 131 lated and presented in Fig. 3 for 50 nm particles, as a function of the magnetic
 132 field strength $\mu_0 H_0$. In the model the magnetisation of the individual nanopar-
 133 ticles is taken as the average value given by the Langevin function. The values
 134 of the capture cross-section predicted through use of the Langevin function

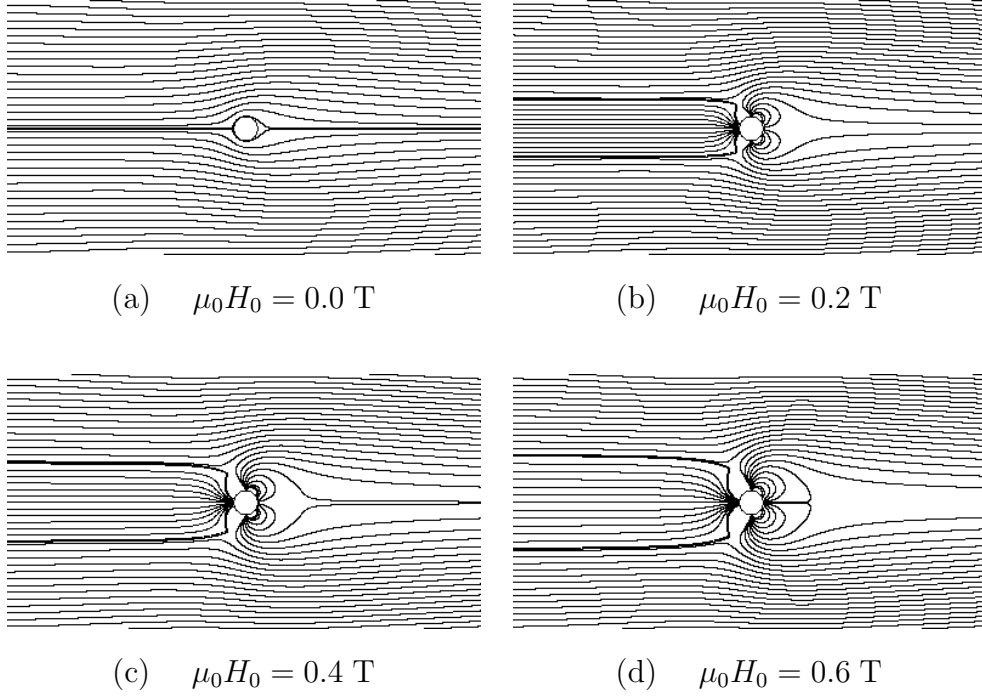


Fig. 2. Streamlines indicating the trajectories of the single domain nanoparticles, calculated using OpenFOAM, as they traverse the control volume for different magnitudes of the externally applied magnetic field, \vec{H}_0 .

135 are significantly larger (see Fig. 3) than would result from the large parti-
 136 cle approach taken by Avilés *et al.*. Beyond a field of $\approx 0.7 \text{ T}$, for the material
 137 used in this simulation, the carrier particle magnetisation is saturated for both
 138 models, leading to identical results.

139 In order to calculate the blood velocity an uniform inlet velocity of 0.1 cm/s
 140 is applied to the model. Other important system and parameters of the fer-
 141 romagnetic materials that are used in the magnetic drug carrier particles and
 142 for the seeds are given in Table 1.

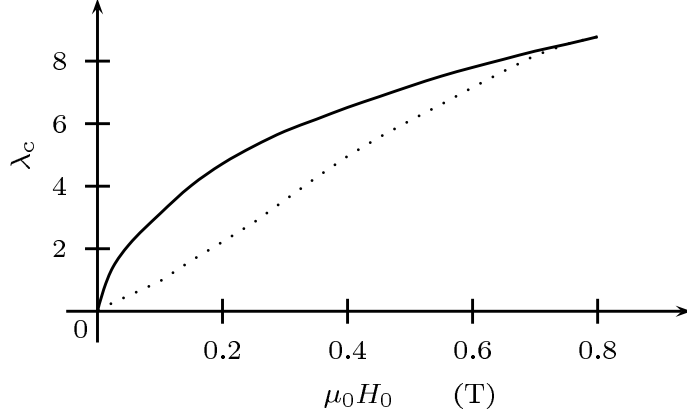


Fig. 3. Capture cross section, λ_c , plotted as a function of the applied magnetic field strength, $\mu_0 H_0$, calculated using (—) the Langevin function as appropriate for single domain particles and (····) without Langevin function as appropriate for multiple domain particles.

Property	Value	SI Unit	Property	Value	SI Unit
ρ_b	1 040.0	kg m^{-3}	$\chi_{\text{seed},0}$	1 000	
η_b	0.002	$\text{kg m}^{-1} \text{s}^{-1}$	$M_{\text{seed},s}$	1 397 000	A m^{-1}
u_0	0.001	m s^{-1}	$M_{\text{fm},p,0,s}$	1 735 000	A m^{-1}
$\mu_0 H_0$	0.0–0.8	$\text{kg s}^{-2} \text{A}^{-1}$	R_s	1.0×10^{-6}	m
$x_{\text{fm},p}$	0		R_p	50×10^{-9}	m
$\rho_{\text{fm},p}$	7 850	kg m^{-3}	$\rho_{\text{pol},p}$	950	kg m^{-3}
$\chi_{\text{fm},p,0}$	1 000				

Table 1

Values of system and material parameters used in the simulation.

143 7 Conclusions

144 The model of Avilés, Ebner and Ritter has been considered for collecting
 145 single domain magnetic drug carrier nanoparticles. Here the Langevin function

146 is used to calculate the expected value of the nanoparticle magnetisation.
147 Magnetic flux density \vec{B} is calculated analytically by using the separation of
148 variable solution and the blood velocity \vec{v}_b is obtained from the Navier-Stokes
149 equation using the finite volume library OpenFOAM. The simulations indicate
150 that use of the Langevin function predicts greater collection efficiency than
151 might be otherwise expected.

152 **8 Acknowledgements**

153 This work was funded by Enterprise Ireland under the Applied Research En-
154 hancement (ARE) program as part of the South Eastern Applied Materials
155 (SEAM) Research Centre at Waterford Institute of Technology. AM is grateful
156 to Cancer Research Ireland (Irish Cancer Society) for an Oncology Scholars
157 Travel Award to attend the 6th *International Conference on the Scientific
158 and Clinical Applications of Magnetic Carriers*, May 2006 in Krems Austria.
159 PJC and AM thank Armin Ebner, Axel Rosengart & Misael Avilés for helpful
160 conversations at Krems.

161 **References**

- 162 [1] Q. A. Pankhurst, J. Connolly, S. K. Jones, J. Dobson, Applications of
163 magnetic nanoparticles in biomedicine, *J. Phys. D: Appl. Phys.* 36 (2003)
164 R167–R181.
- 165 [2] C. C. Berry, A. S. G. Curtis, Functionalisation of magnetic nanoparticles
166 for applications in biomedicine, *J. Phys. D: Appl. Phys.* 36 (2003) R198–
167 R206.

- 168 [3] A. D. Grief, G. Richardson, Mathematical modelling of magnetically tar-
169 geted drug delivery, *J. Magn Magn Mater.* 293 (1) (2005) 455–463.
- 170 [4] G. Iacob, O. Rotariu, N. J. C. Strachan, U. O. Häfeli, Magnetizable nee-
171 dles and wires - modeling an efficient way to target magnetic microspheres
172 in vivo, *Biorheology* 41 (2004) 599–612.
- 173 [5] J. A. Ritter, A. D. Ebner, K. D. Daniel, K. L. Stewart, Application of
174 high gradient magnetic separation principles to magnetic drug targeting,
175 *J. Magn Magn Mater.* 280 (2-3) (2004) 184–201.
- 176 [6] M. O. Avilés, A. D. Ebner, H. Chen, A. J. Rosengart, M. D. Kaminski,
177 J. A. Ritter, Theoretical analysis of a transdermal ferromagnetic implant
178 for retention of magnetic drug carrier particles, *J. Magn Magn Mater.*
179 293 (1) (2005) 605–615.
- 180 [7] H. Chen, A. D. Ebner, M. D. Kaminski, A. J. Rosengart, J. A. Rit-
181 ter, Analysis of magnetic drug carrier particle capture by a magnetizable
182 intravascular stent: Parametric study with multi-wire two-dimensional
183 model, *J. Magn Magn Mater.* 293 (1) (2005) 616–632.
- 184 [8] B. B. Yellen, Z. G. Forbes, D. S. Halverson, G. Fridman, K. A. Barbee,
185 M. Chorny, R. Levy, G. Friedman, Targeted drug delivery to magnetic im-
186 plants for therapeutic applications, *J. Magn Magn Mater.* 293 (1) (2005)
187 647–654.
- 188 [9] E. J. Furlani, E. P. Furlani, A model for predicting magnetic targeting of
189 multifunctional particles in the microvasculature, *J. Magn Magn Mater.*
190 312 (1) (2007) 187–193.
- 191 [10] M. O. Avilés, A. D. Ebner, J. A. Ritter, Ferromagnetic seeding for the
192 magnetic targeting of drugs and radiation in capillary beds, *J. Magn
193 Magn Mater.* 310 (1) (2007) 131–144.

- 194 [11] M. I. Shliomis, Magnetic fluids, *Sov. Phys. Usp.* 17 (3) (1974) 153–169.
- 195 [12] H. C. Bryant, D. A. Sergatskov, D. Lovato, N. L. Adolphi, R. S. Larson,
196 E. R. Flynn, Magnetic needles and superparamagnetic cells, *Phys. Med.*
197 *Biol.* 52 (14) (2007) 4009–4025.
- 198 [13] OpenCFD Ltd, OpenFOAM 1.4, <http://www.opencfd.co.uk> (2007).